ACS chemical biology

Letters

pubs.acs.org/acschemicalbiology

Human Haploid Cell Genetics Reveals Roles for Lipid Metabolism Genes in Nonapoptotic Cell Death

Scott J. Dixon,*[,†,⊥,#] Georg E. Winter,[‖,#] Leila S. Musavi,[†] Eric D. Lee,[†] Berend Snijder,[‖] Manuele Rebsamen,[‖] Giulio Superti-Furga,*[,‖] and Brent R. Stockwell*[,†,‡,§]

[†]Department of Biological Sciences, [‡]Department of Chemistry, and [§]Howard Hughes Medical Institute, Columbia University, 550 West 120th Street, Northwest Corner Building, MC 4846, New York, New York 10027, United States

[‖]CeMM Research Center for Molecular Medicine of the Austrian Academy of Sciences, Lazarettgasse 14, 1090 Vienna, Austria

[⊥]Department of Biology, Stanford University, 337 Campus Drive, Stanford, California 94305, United States

Supporting Information

ABSTRACT: Little is known about the regulation of nonapoptotic cell death. Using massive insertional mutagenesis of haploid KBM7 cells we identified nine genes involved in small-molecule-induced nonapoptotic cell death, including mediators of fatty acid metabolism (*ACSL4*) and lipid remodeling (*LPCAT3*) in ferroptosis. One novel compound, CIL56, triggered cell death dependent upon the rate-limiting *de novo* lipid synthetic enzyme ACC1. These results provide insight into the genetic regulation of cell death and highlight the central role of lipid metabolism in nonapoptotic cell death.

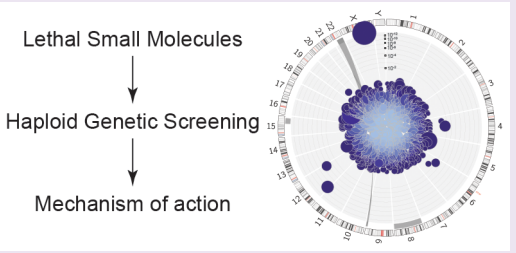

Several nonapoptotic, regulated cell death (RCD) pathways have been discovered in recent years, including necroptosis, pyroptosis and ferroptosis.[1] These pathways have been implicated in a variety of pathological conditions, and small molecules that can activate or inhibit nonapoptotic cell death have emerged as important therapeutic leads for a variety of diseases.[1−3]

Ferroptosis is an iron-dependent form of RCD observed in cancer cells, kidney cells and neurons.[4−8] Ferroptosis can be caused by inhibition of system x_c^- or glutathione peroxidase 4 (GPX4).[9,10] System x_c^- is required to import cystine into cells for glutathione synthesis, and GPX4 uses glutathione to detoxify lipid peroxides. Erastin is a system x_c^- inhibitor, while (1*S*,3*R*)-RSL3 (hereafter RSL3) and ML162 (also known as DPI7) inactivate GPX4.[9,10] The genetic networks regulating sensitivity to these and other death-inducing compounds are not well-defined.

Defining small molecule mechanism of action is challenging.[11,12] One potential approach employs a nearly haploid chronic myeloid leukemia cell line, KBM7, coupled with retroviral-mediated insertional mutagenesis and sequencing to identify genes required for lethality.[13−15] This approach has been used to investigate the lethal mechanism of action of tunicamycin, 3-bromopyruvate and YM155 and, in each case, has identified a specific transporter protein necessary for the cellular uptake of each of these lethal compounds.[15−17] We sought to apply this approach to identify genes involved in ferroptosis and other forms of nonapoptotic RCD.

We examined the mechanism of action of five small molecules that trigger nonapoptotic cell death: erastin, RSL3, ML162, PK-3,[18] and a novel compound, CIL56[19] (Figure 1a). As a control, we examined the apoptosis-inducing small molecule BH3 mimetic ABT-263. Based on previous results using a related analogue, ABT-737,[14] we expected to identify insertions into BCL2-associated X protein (*BAX*) and phorbol-12-myristate-13-acetate-induced protein 1 (*PMAIP1/NOXA*) as suppressors of ABT-263-induced death if our screening system was performing as desired.

All six test compounds were lethal to KBM7 cells, with erastin, RSL3, and ML162 inducing ferroptosis, as judged by the ability of the lipophilic antioxidant ferrostatin-1 (Fer-1) and the iron chelator ciclopirox olamine (CPX) to prevent death[4] (Figure 1b). The lethality of erastin was also suppressed by the reducing agent beta-mercaptoethanol (β-ME), as expected for a system x_c^- inhibitor[4] (Figure 1b). The lethality of ABT-263 was not suppressed by Fer-1, CPX, or β-ME, as expected for an apoptosis-inducing agent. In these experiments, neither PK-3 nor CIL-56 induced ferroptosis; other results[18,19] suggest that these compounds induce unknown forms of nonapoptotic cell death. Indeed, an important goal of these studies was to identify genes that might distinguish the lethal pathways activated by these compounds.

Screening trials identified compound concentrations yielding resistant colonies for PK-3 (55 nM), ML162 (9 μM), RSL3 (4 μM), CIL56 (5.5 μM), and ABT-263 (2.5 μM). For erastin, none of the tested lethal concentrations yielded any resistant colonies, suggesting that cystine import via system x_c^- is unconditionally essential for colony formation and can not be compensated for by the deletion of any single gene; this finding

Received: April 6, 2015
Accepted: May 12, 2015

DOI: 10.1021/acschembio.5b00245
ACS Chem. Biol. XXXX, XXX, XXX−XXX

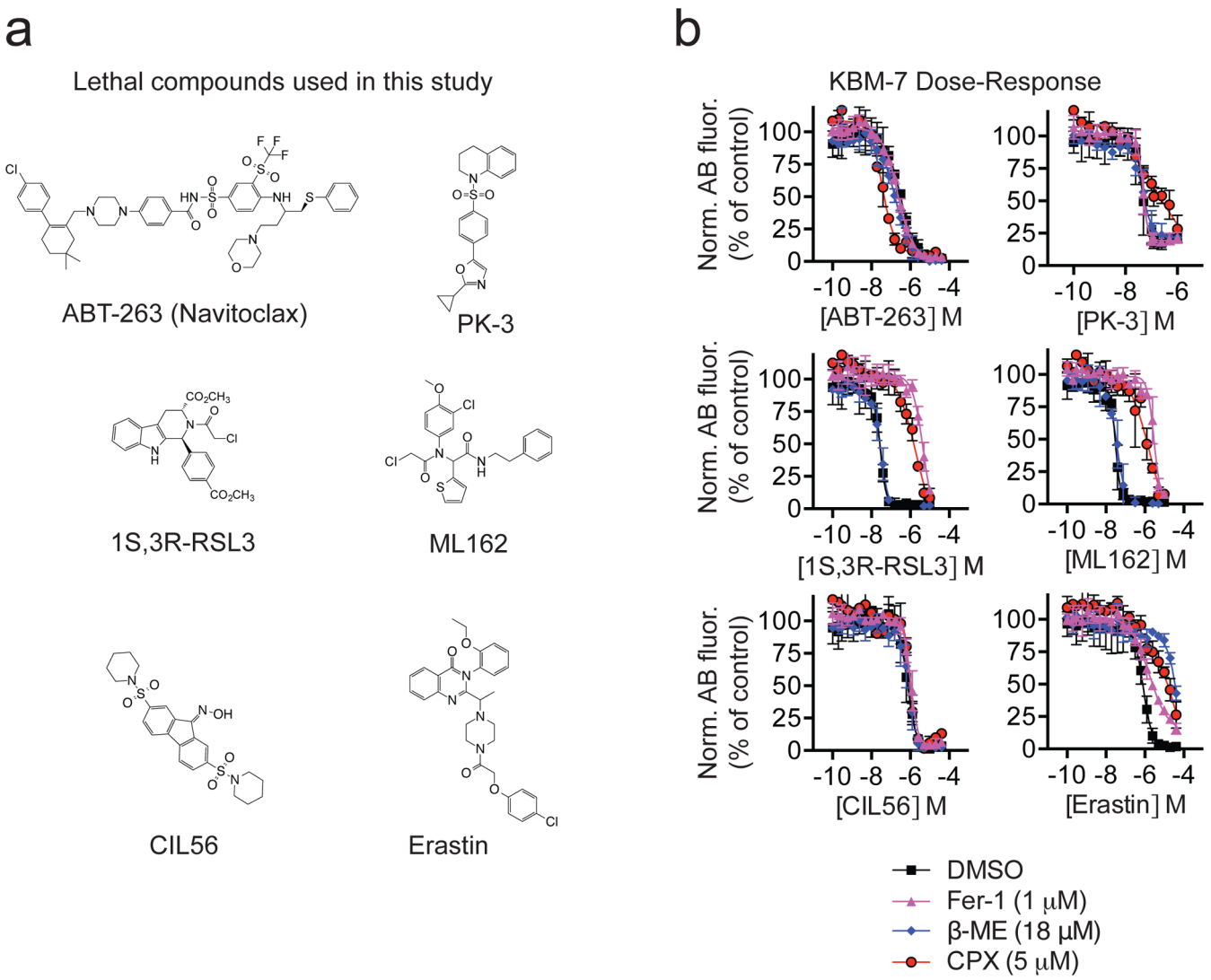

Figure 1. Effect of lethal molecules in KBM7 cells. (a) Structure of the lethal molecules tested in this study. (b) Dose−response analysis of seven lethal compounds in KBM7 cells ± three ferroptosis inhibitors ferrostatin-1 (Fer-1), beta-mercaptoethanol (β-ME), and ciclopirox olamine (CPX). Norm. AB Fluor.: Normalized Alamar Blue Fluorescence, an indication of cell viability. Data represents the mean ± SD from three independent biological replicates.

suggests that tumors might find it difficult to evolve resistance to system x_c^- inhibitors through gene deletion.

The five remaining compounds were individually added to an initial pool of 1×10^8 KBM7 cells that were heavily mutagenized using a retroviral genetrap vector, as described previously.[14] After compound incubation for 10 to 21 days, resistant colonies were collected and retroviral insertion sites mapped to individual genes[14] (Figure 2). Not shown are insertions into three genes: *NF1*, *WT1* and *SPI1*, which were commonly identified in most screens, suggesting that they may confer a general drug-resistant phenotype when mutated in KBM7 cells.

As expected,[14] ABT-263-resistant cells had a significant overrepresentation of insertions in *BAX* ($P < 10^{-50}$) and *PMAIP1/NOXA* ($P = 5.5 \times 10^{-39}$) (Figure 2a). We confirmed that clonal KBM7 cell lines lacking either gene were resistant to ABT-263 (Supplemental Figure 1). These results provided confidence in our ability to identify genes required for small molecule-induced cell death using this approach. Unexpectedly, the analysis of PK-3-resistant colonies yielded no significantly enriched genes (Figure 2b). PK-3 binds tubulin and disrupts the intracellular microtubule network, which is necessary for mitosis.[18] We speculate that PK-3-resistant colonies could arise in the absence of specific mutations from a transient subpopulation of nondividing (i.e., quiescent, G_0) cells. Transcriptional upregulation of genes encoding xenobiotic detoxification enzymes or drug pumps in these cells could then allow for survival and subsequent proliferation in the presence of PK-3. Further analysis of additional microtubule-disrupting agents in KBM-7 cells would help resolve this issue.

We next analyzed RSL3 and ML162, two structurally distinct compounds that both inhibit GPX4.[10] Analysis of RSL3-resistant cells identified four genes significantly enriched for gene trap insertions: acyl-CoA synthetase long-chain family member 4 (*ACSL4*, $P = 3.5 \times 10^{-259}$), lysophosphatidylcholine acyltransferase 3 (*LPCAT3*, $P = 3.0 \times 10^{-107}$), 1-acylglycerol-3-phosphate *O*-acyltransferase 3 (*AGPAT3*, $P = 6.2 \times 10^{-16}$), and hydroxysteroid (17-beta) dehydrogenase 11 (*HSD17B11*, $P = 5.8 \times 10^{-9}$) (Figure 2c). Analysis of ML162-resistant cells identified three genes significantly enriched for insertions, two of which were shared with RSL3 (*ACSL4* and *LPCAT3*, *P* values of 5.7×10^{-20} and 7.1×10^{-11}), and one of which was

DOI: 10.1021/acschembio.5b00245
ACS Chem. Biol. XXXX, XXX, XXX−XXX

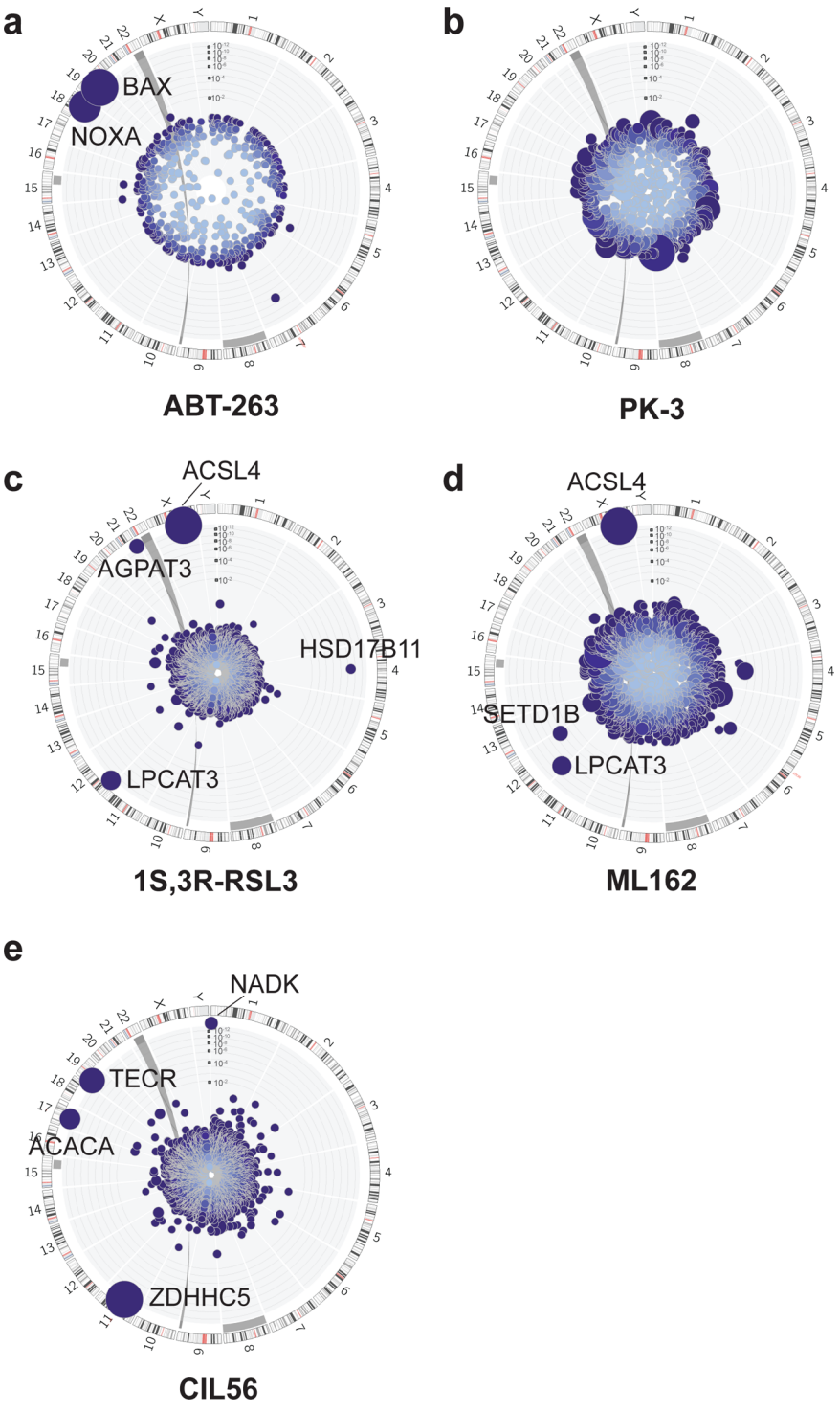

Figure 2. Identifying genetic determinants of small molecule lethality. (a–e) Circos Plots for each lethal compound showing every gene with at least one mapped retroviral insertion represented as a blue circle oriented toward the chromosomal position of the gene. Circle size is proportional to the number of insertions, and distance from the center is proportional to the significance (p-value) of this number of insertions relative to control cells. Genes enriched in selected versus unselected pools with p-values < 10^{-3} are indicated.

unique, but less significantly enriched (SET domain containing 1B, *SETD1B*, $P = 1.9 \times 10^{-4}$) (Figure 2d). The overlap of *ACSL4* and *LPCAT3* between RSL3 and ML162 provides confidence that these two genes are essential for the execution of ferroptosis induced by inhibition of GPX4.

Cells undergoing ferroptosis are depleted of arachidonic acid (AA, 20:4) and other polyunsaturated fatty acids (PUFAs).[5,7] The prevailing model is that the oxidative destruction of PUFAs, following GPX4 inactivation, is essential for the execution of ferroptosis.[5,7] ACSL4 preferentially acylates AA,[20] while LPCAT3 preferentially catalyzes the insertion of acylated AA into membrane phospholipids.[21] Thus, deletion of *ACSL4* and *LPCAT3* likely suppress ferroptosis by limiting the membrane-resident pool of oxidation-sensitive fatty acids. Further studies will be required to elucidate the roles of *AGPAT3*, *HSD17B11*, and *SETD1B* and determine if the

DOI: 10.1021/acschembio.5b00245
ACS Chem. Biol. XXXX, XXX, XXX–XXX

identification of these genes in only the RLS3 (*HSD17B11*, *AGPAT3*) or the ML162 (*SETD1B*) screens reflects the existence of false negatives unique to each screen, or to true biological differences in the lethal effects of these two compounds.

Finally, we analyzed results obtained with CIL56 and identified a unique set of significantly enriched genes compared to ABT-263, RSL3, and ML162, including zinc finger, DHHC domain containing 5 (*ZDHHC5*, $P = 6.3 \times 10^{-218}$), *trans*-2,3-enoyl-CoA reductase (*TECR*, $P = 1.2 \times 10^{-131}$), acetyl-CoA carboxylase alpha (*ACACA*, $P = 3.6 \times 10^{-56}$, individual insertions sites into this gene shown in Supplemental Figure 3a), and NAD kinase (NADK, $P = 8.8 \times 10^{-31}$) (Figure 2e). *ACACA* (encoding ACC1) is a key regulator of tumor cell survival,[22] and we therefore focused on the role of ACC1 in CIL56-induced death.

ACC1 catalyzes the conversion of acetyl-CoA to malonyl-CoA, the rate-limiting step in fatty acid synthesis (Figure 3a). Two clonal *ACACA* null HT-1080 cells lines (H and P), which we generated using CRISPR/Cas9 technology, lacked ACC1 expression and exhibited 5-fold resistance to CIL56, but no consistent resistance to RSL3 or the apoptosis-inducing agents hydrogen peroxide (H_2O_2) or staurosporine (STS) (Figure 3b–f, Supplemental Figure 2b). Silencing of *ACACA* in HT-1080 cells using two independent siRNAs likewise resulted in resistance toward CIL56, but not RSL3 (Supplemental Figure 2c–e). Furthermore, the lethality of CIL56, but not RSL3 or erastin, was suppressed by the small molecule ACC1 inhibitor 5-tetradecyloxy-2-furonic acid (TOFA)[22,23] (Figure 3g). Conversely, cell death induced by erastin and RSL3, but not CIL56, was suppressed by Fer-1 (Figure 3g). These results suggest that ACC1 activity sensitizes cells to CIL56-induced cell death.

Using mass spectrometry, we analyzed the metabolome of HT-1080 cells treated with CIL56 (6.5 μM) ± TOFA (4 μM), compared to vehicle-treated controls. Among the 298 polar and nonpolar metabolites identified in this analysis, the levels of 141 metabolites were significantly altered by CIL56 treatment, with 82 metabolites significantly increased and 59 significantly decreased (FDR $q < 0.01$) (Figure 3h, Supplemental Table 1). In cells cotreated with CIL56 and TOFA, we detected no significantly altered metabolites compared to vehicle-treated cells (at FDR $q < 0.01$) (Figure 3h, Supplemental Table 1). This suggested that the effects of CIL56 on metabolism were completely reversed by TOFA. Of note, CIL56 triggered the striking TOFA-sensitive accumulation of all detectable long chain saturated and monounsaturated fatty acids and all detectable polyunsaturated fatty acids (Figure 3i,j and Supplemental Table 1). A plausible model to account for the accumulation of both nonessential and essential fatty acids species is that CIL56 inhibits the normal breakdown of fatty acids by mitochondrial β-oxidation. This could occur if, for example, CIL56 accelerated the ACC1-dependent production of malonyl-CoA, a metabolite that acts as a negative regulator of this process.[24] While it remains possible that CIL56 could engage more than one target, our results are consistent with the model that CIL56 stimulates the activity of ACC1 itself, or an upstream component of the fatty acid synthesis pathway, to cause cell death. One prediction of this model is that overexpression of ACC1 might sensitize to CIL56-induced death, although regulation of ACC1 and downstream lipid synthetic enzymes may be sufficiently complex to preclude this.[25]

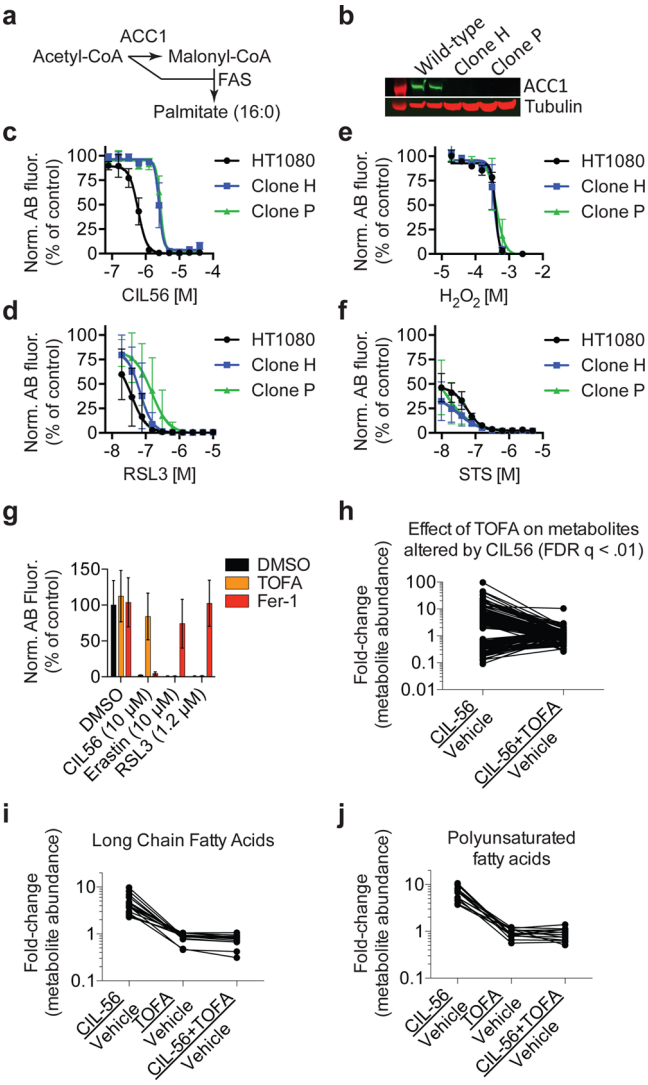

Figure 3. Analysis of the role of *ACACA* in CIL56-induced death. (a) The role of ACC1 (encoded by *ACACA*) in fatty acid synthesis. FAS: fatty acid synthase. (b) Western blot of ACC1 levels in two independent HT-1080 cell clones (H and P). Each lysate was loaded twice in adjacent lanes. (c–f) Viability of HT-1080 cells and variants lacking ACC1 treated with various lethal compounds. (g) Viability of HT-1080 cells treated for 24 h with lethal compounds ± TOFA (5 μM) or Fer-1 (1 μM). Norm. AB Fluor.: Normalized Alamar Blue Fluorescence, an indication of cell viability. (h–j) Metabolomic analysis of HT-1080 cells treated with CIL56 (6.5 μM) ± TOFA (4 μM). (h) Fold-change in abundance of 144 metabolites significantly altered by CIL56 treatment (FDR $q < 0.01$) ± TOFA. (i) Fold-change in metabolite levels for saturated fatty acids. (j) Fold-change in metabolite levels for polyunsaturated fatty acids.

Together, these results implicate the lipid metabolic genes *ACSL4* and *LPCAT3* in ferroptosis and *ACACA* in the novel cell death program triggered by CIL56. It remains unclear how CIL56 treatment causes cell death, although the accumulation of saturated fatty acids[26] or the inhibition of mitochondrial β-oxidation could be involved. An important aim of future studies will be to pinpoint the specific molecular changes that are responsible for CIL56-induced cell death. Future studies using clonal cell lines lacking the lipid metabolic enzymes identified here should greatly facilitate this process.

DOI: 10.1021/acschembio.5b00245
ACS Chem. Biol. XXXX, XXX, XXX–XXX

METHODS

Materials. Erastin,[27] 1*S*,3*R*-RSL3,[10] and ferrostatin-1[5] were synthesized as described; PK-3 was identified from a library of small molecules.[18] Tetradecyloxy-2-furonic acid was obtained from Santa Cruz Biotechnology. Unless indicated, all other compounds were obtained from Sigma.

Tissue Culture. KBM7 cells were cultured as described.[15] HT-1080 cells were obtained from American Type Culture Collection and grown in DMEM High-Glucose media (Gibco) supplemented with 10% FBS, 1% nonessential amino acids (Gibco), and 1% penicillin and streptomycin (Gibco). Cell were grown in humidified tissue culture incubators (Thermo Scientific) at 37 °C with 5% CO_2.

Haploid Genetic Screening. Haploid genetic screening was conducted as described.[13] In brief, virus was produced by transient transfection of the gene-trap plasmid along with packaging plasmids using Lipofectamine 2000 (Invitrogen) in low-passage HEK 293T cells. Virus was concentrated via ultracentrifugation and used to mutagenize 1×10^8 KBM7 cells via spinfection. Mutagenized cells were then expanded and either directly used for genetic screens (ABT-263, CIL56) or screened after one freeze−thaw cycle. Drug concentrations were titrated to allow outgrowth of approximately 1000 to 10 000 colonies per screen. Of note, in order to facilitate the outgrowth of drug-tolerant clones, drug effects were diluted out after 3 days of initial incubation with growth medium yielding estimated final concentrations of 833 nM (ABT-263), 18 nM (PK-3), 1.83 μM (CIL56), 3 μM (ML162), and 1.33 μM (RSL3). Gene trapped cells were selected with the indicated drug concentrations in 96 well plates (1×10^5 cells seeded/well). Drug-resistant clones were pooled after indicated time-points, collected in a T175 flask and expanded to a total cell number of 3×10^7 cells. Genomic DNA was isolated and retroviral insertion sites were detected via an inverse PCR protocol adopted to next generation sequencing.[14] The significance of the enrichment of insertions in a given gene was calculated by comparing the number of insertions of the respective drug selected population with an unselected, larger control data set using the one-sided Fisher's exact test. The resulting *p*-values were false-discovery rate corrected accordingly.

CRISPR/Cas9 Genome Editing. HT-1080 cells were transfected with a plasmid encoding Cas9 and short guide RNAs (sgRNAs) targeting exon 4 of *ACACA* and a second plasmid encoding turboGFP (Evrogen). Two days later, individual cells were sorted by flow cytometry into separate wells of a 96-well plate. Following colony outgrowth, individual clones were screened for resistance to CIL56. Two clones (H and P) were identified by this procedure. For these clones, cells were grown in 6-well dishes and genomic DNA was purified using the QIAamp DNA Mini Kit (Qiagen). Primers flanking exon 4 of *ACACA* were used in a PCR reaction with Taq DNA Polymerase (Life Technologies). Samples were separated with agarose gel electrophoresis. The amplified target DNA was cut out of the gel and purified using the QIAquick Gel Extraction Kit. Purified DNA samples were sent to GeneWiz, Inc., for sequencing.

Western Blotting. HT-1080 cells were seeded in 6-well dishes at 300 000 cells/well in regular HT-1080 media 24 h prior to use. Cells were washed twice with PBS and lysed in 75 μL buffer [50 mM HEPES, 40 mM NaCl, 2 mM EDTA, 0.5% Triton-X, 1.5 mM sodium orthovanadate, 50 mM NaF, 10 mM sodium pyrophosphate, 10 mM sodium β-glycerophosphate, and protease inhibitor tablet (Roche), pH 7.4]. Lysates were pelleted for ten min at 12 000 rpm at 4 °C. Samples were separated using SDS-polyacrylamide gel electrophoresis and transferred to a polyvinylidene difluoride membrane (Invitrogen) using the iBlot system (Invitrogen). Membranes were blocked in Li-COR Odyssey blocking buffer for 1 h at 25 °C, then incubated with primary antibodies (1:1000) in a 1:1 solution of PBS-T and blocking buffer overnight at 4 °C. Following three 5 min washes in PBS-T, the membrane was incubated with secondary antibodies (1:1000) in a 1:1 solution of PBS-T and blocking buffer for 1 h at 25 °C protected from light. Following three 5 min washes in PBS-T, the membrane was scanned using the Li-COR Odyssey Imaging System. Monoclonal antibodies for ACC1 (Life Technologies) and tubulin (Cell Signaling Technology) were detected using a goat antirabbit or goat antimouse IgG antibody, conjugated with IRdye 800 CW or 680 CW, respectively (Li-COR Biosciences).

siRNA Reverse Transfection. HT-1080 cells were reverse transfected with siRNAs (Qiagen) using Lipofectamine RNAiMAX (LFMax, Invitrogen) as described.[9] Briefly, 10 nM (final concentration) of siRNAs were aliquoted into 250 μL of Opti-MEM media (Gibco) in the bottom of each well of a 6-well dish (Corning). An additional 250 μL of media + LFMax was added to each well and incubated for 15 min. Next, 150 000 HT-1080 cells were added to each well in regular HT-1080 media. The plates were swirled to mix and incubated for 48 h at 37 °C in a tissue culture incubator prior to analysis.

Cell Viability Measurements. Cell viability was assessed in 384-well format by Alamar Blue (Invitrogen) fluorescence (ex/em 530/590) measured on a Victor3 platereader (PerkinElmer).

Metabolite Profiling. Metabolite profiling was performed by Metabolon. HT-1080 cells were treated with CIL56 and/or TOFA for 8 h and samples were collected and processed as described previously.[5]

ASSOCIATED CONTENT

Supporting Information

Supplemental Figures 1 and 2 and Table 1. The Supporting Information is available free of charge on the ACS Publications website at DOI: 10.1021/acschembio.5b00245.

AUTHOR INFORMATION

Corresponding Authors

*E-mail: sjdixon@stanford.edu.
*E-mail: gsuperti-furga@cemm.oeaw.ac.at.
*E-mail: bstockwell@columbia.edu.

Author Contributions

#These authors contributed equally to this work.

Notes

The authors declare no competing financial interest.

ACKNOWLEDGMENTS

We thank T. Brummelkamp for providing the KBM7 clones deficient in the expression of BAX and PMAIP1, as well as for experimental advice. This work was supported by an R00 Award from the National Cancer Institute to S.J.D (4R00CA166517-03). B.R.S. is an Early Career Scientist of the Howard Hughes Medical Institute and is supported by grants from the US National Institute of Health (5R01CA097061, 5R01GM085081, and R01CA161061) and NYSTEM. Work in the G.S.-F. laboratory was supported by the Austrian Academy of Sciences and to Swiss NSF fellowships to B.S.

REFERENCES

(1) Vanden Berghe, T., Linkermann, A., Jouan-Lanhouet, S., Walczak, H., and Vandenabeele, P. (2014) Regulated necrosis: the expanding network of non-apoptotic cell death pathways. *Nat. Rev. Mol. Cell Biol. 15*, 135−147.

(2) Linkermann, A., Stockwell, B. R., Krautwald, S., and Anders, H.-J. (2014) Regulated cell death and inflammation: an auto-amplification loop causes organ failure. *Nat. Rev. Immunol. 14*, 759−767.

(3) Dixon, S. J., and Stockwell, B. R. (2014) The role of iron and reactive oxygen species in cell death. *Nat. Chem. Biol. 10*, 9−17.

(4) Dixon, S. J., Lemberg, K. M., Lamprecht, M. R., Skouta, R., Zaitsev, E. M., Gleason, C. E., Patel, D. N., Bauer, A. J., Cantley, A. M., Yang, W. S., Morrison, B., and Stockwell, B. R. (2012) Ferroptosis: an iron-dependent form of nonapoptotic cell death. *Cell 149*, 1060−1072.

(5) Skouta, R., Dixon, S. J., Wang, J., Dunn, D. E., Orman, M., Shimada, K., Rosenberg, P. A., Lo, D. C., Weinberg, J. M., Linkermann,

DOI: 10.1021/acschembio.5b00245
ACS Chem. Biol. XXXX, XXX, XXX−XXX

A., and Stockwell, B. R. (2014) Ferrostatins inhibit oxidative lipid damage and cell death in diverse disease models. *J. Am. Chem. Soc. 136*, 4551−4556.
(6) Linkermann, A., Skouta, R., Himmerkus, N., Mulay, S. R., Dewitz, C., De Zen, F., Prokai, A., Zuchtriegel, G., Krombach, F., Welz, P.-S., Weinlich, R., Vanden Berghe, T., Vandenabeele, P., Pasparakis, M., Bleich, M., Weinberg, J. M., Reichel, C. A., Bräsen, J. H., Kunzendorf, U., Anders, H.-J., Stockwell, B. R., Green, D. R., and Krautwald, S. (2014) Synchronized renal tubular cell death involves ferroptosis. *Proc. Natl. Acad. Sci. U.S.A. 111*, 16836−16841.
(7) Friedmann Angeli, J. P., Schneider, M., Proneth, B., Tyurina, Y. Y., Tyurin, V. A., Hammond, V. J., Herbach, N., Aichler, M., Walch, A., Eggenhofer, E., Basavarajappa, D., Rådmark, O., Kobayashi, S., Seibt, T., Beck, H., Neff, F., Esposito, I., Wanke, R., Förster, H., Yefremova, O., Heinrichmeyer, M., Bornkamm, G. W., Geissler, E. K., Thomas, S. B., Stockwell, B. R., O'Donnell, V. B., Kagan, V. E., Schick, J. A., and Conrad, M. (2014) Inactivation of the ferroptosis regulator Gpx4 triggers acute renal failure in mice. *Nat. Cell Biol. 16*, 1180−1191.
(8) Jiang, L., Kon, N., Li, T., Wang, S.-J., Su, T., Hibshoosh, H., Baer, R., and Gu, W. (2015) Ferroptosis as a p53-mediated activity during tumour suppression. *Nature 520*, 57−62.
(9) Dixon, S. J., Patel, D. N., Welsch, M., Skouta, R., Lee, E. D., Hayano, M., Thomas, A. G., Gleason, C. E., Tatonetti, N. P., Slusher, B. S., and Stockwell, B. R. (2014) Pharmacological inhibition of cystine-glutamate exchange induces endoplasmic reticulum stress and ferroptosis. *eLife 3*, e02523.
(10) Yang, W. S., SriRamaratnam, R., Welsch, M. E., Shimada, K., Skouta, R., Viswanathan, V. S., Cheah, J. H., Clemons, P. A., Shamji, A. F., Clish, C. B., Brown, L. M., Girotti, A. W., Cornish, V. W., Schreiber, S. L., and Stockwell, B. R. (2014) Regulation of ferroptotic cancer cell death by GPX4. *Cell 156*, 317−331.
(11) Schenone, M., k, V. D. C. I., Wagner, B. K., and Clemons, P. A. (2013) Target identification and mechanism of action in chemical biology and drug discovery. *Nat. Chem. Biol. 9*, 232−240.
(12) Lee, J., and Bogyo, M. (2013) Target deconvolution techniques in modern phenotypic profiling. *Curr. Opin. Chem. Biol. 17*, 118−126.
(13) Carette, J. E., Guimaraes, C. P., Varadarajan, M., Park, A. S., Wuethrich, I., Godarova, A., Kotecki, M., Cochran, B. H., Spooner, E., Ploegh, H. L., and Brummelkamp, T. R. (2009) Haploid genetic screens in human cells identify host factors used by pathogens. *Science 326*, 1231−1235.
(14) Carette, J. E., Guimaraes, C. P., Wuethrich, I., Blomen, V. A., Varadarajan, M., Sun, C., Bell, G., Yuan, B., Muellner, M. K., Nijman, S. M., Ploegh, H. L., and Brummelkamp, T. R. (2011) Global gene disruption in human cells to assign genes to phenotypes by deep sequencing. *Nat. Biotechnol. 29*, 542−546.
(15) Winter, G. E., Radic, B., Mayor-Ruiz, C., Blomen, V. A., Trefzer, C., Kandasamy, R. K., Huber, K. V. M, Gridling, M., Chen, D., Klampfl, T., Kralovics, R., Kubicek, S., Fernandez-Capetillo, O., Brummelkamp, T. R., and Superti-Furga, G. (2014) The solute carrier SLC35F2 enables YM155-mediated DNA damage toxicity. *Nat. Chem. Biol. 10*, 768−773.
(16) Birsoy, K., Wang, T., Possemato, R., Yilmaz, O. H., Koch, C. E., Chen, W. W., Hutchins, A. W., Gultekin, Y., Peterson, T. R., Carette, J. E., Brummelkamp, T. R., Clish, C. B., and Sabatini, D. M. (2013) MCT1-mediated transport of a toxic molecule is an effective strategy for targeting glycolytic tumors. *Nat. Genet. 45*, 104−108.
(17) Reiling, J. H., Clish, C. B., Carette, J. E., Varadarajan, M., Brummelkamp, T. R., and Sabatini, D. M. (2011) A haploid genetic screen identifies the major facilitator domain containing 2A (MFSD2A) transporter as a key mediator in the response to tunicamycin. *Proc. Natl. Acad. Sci. U.S.A. 108*, 11756−11765.
(18) Yang, W. S., Shimada, K., Delva, D., Patel, M., Ode, E., Skouta, R., and Stockwell, B. R. (2012) Identification of simple compounds with microtubule-binding activity that inhibit cancer cell growth with high potency. *ACS Med. Chem. Lett. 3*, 35−38.
(19) Shimada, K.; Skouta, R.; Yang, W. S.; Hayano, M.; Dixon, S. J.; Patel, D. N.; et al. Unpublished data.
(20) Soupene, E., and Kuypers, F. A. (2008) Mammalian long-chain acyl-CoA synthetases. *Exp. Biol. Med. 233*, 507−521.
(21) Shindou, H., and Shimizu, T. (2009) Acyl-CoA:lysophospholipid acyltransferases. *J. Biol. Chem. 284*, 1−5.
(22) Jeon, S.-M., Chandel, N. S., and Hay, N. (2012) AMPK regulates NADPH homeostasis to promote tumour cell survival during energy stress. *Nature 485*, 661−665.
(23) McCune, S. A., and Harris, R. A. (1979) Mechanism responsible for 5-(tetradecyloxy)-2-furoic acid inhibition of hepatic lipogenesis. *J. Biol. Chem. 254*, 10095−10101.
(24) Abu-Elheiga, L., Matzuk, M. M., Abo-Hashema, K. A., and Wakil, S. J. (2001) Continuous fatty acid oxidation and reduced fat storage in mice lacking acetyl-CoA carboxylase 2. *Science 291*, 2613−2616.
(25) Moon, Y.-A., and Horton, J. D. (2003) Identification of two mammalian reductases involved in the two-carbon fatty acyl elongation cascade. *J. Biol. Chem. 278*, 7335−7343.
(26) Listenberger, L. L., Han, X., Lewis, S. E., Cases, S., Farese, R. V., Ory, D. S., and Schaffer, J. E. (2003) Triglyceride accumulation protects against fatty acid-induced lipotoxicity. *Proc. Natl. Acad. Sci. U.S.A. 100*, 3077−3082.
(27) Yagoda, N., von Rechenberg, M., Zaganjor, E., Bauer, A. J., Yang, W. S., Fridman, D. J., Wolpaw, A. J., Smukste, I., Peltier, J. M., Boniface, J. J., Smith, R., Lessnick, S. L., Sahasrabudhe, S., and Stockwell, B. R. (2007) RAS-RAF-MEK-dependent oxidative cell death involving voltage-dependent anion channels. *Nature 447*, 864−868.

DOI: 10.1021/acschembio.5b00245
ACS Chem. Biol. XXXX, XXX, XXX−XXX